EurJIC
European Journal of Inorganic Chemistry

Research Article
doi.org/10.1002/ejic.202400408

Chemistry Europe
European Chemical Societies Publishing

www.eurjic.org

A Macrocycle with a Pair of Endo-Isocyanides and its Affinity to Gold(I)

Charlotte Kress,[a] Daniel Häussinger,[a] Patrick Zwick,[a] Alessandro Prescimone,[a] and Marcel Mayor*[a, b, c]

A pair of isocyanides pointing towards each other are fixed in a macrocyclic scaffold. The arrangement not only increases their local concentration, it should also enable their linear arrangement in coordination compounds. The macrocyclic diisocyanide ligand **1** is synthesized and fully characterized. Its interaction with gold(I) ions is investigated. While IR- and ^{1}H-NMR-based titration experiments unraveled a stoichiometry of 2 Au(I) ions per macrocycle **1**, the corresponding association constants are studied by UV-Vis titration experiments. However, the values are above the method's detection limits and only a lower boundary of an over-all association constant is determined to be 3.0×10^{7} M^{-1}. The kinetics of the complex formation is further analyzed by NMR titration experiments and in spite of a change in the solvent, association constants about one order of magnitude larger than the lower limit determined by the UV-Vis experiments are obtained.

Introduction

Isocyanide as wide spread and versatile functional group appears in numerous research areas ranging among others from catalysis,[1,2] diagnostic medicine,[1,3] surface chemistry,[1,4,5] and photochemistry,[6–8] to molecular electronics.[9–11] In particular, the lone pair on the carbon atom[12,13] allows to perform multi step reactions[2,13] and is of interest for the formation of complexes with metal ions resulting in an organometallic carbon-to-metal bond.[3,12,14]

The isocyanide is characterized by the nitrogen to carbon triple bond with a length of 1.167 Angstrom (Å)[3,15] and a dihedral angle of 180°.[3,12–15] These properties result in a characteristic infra–red (IR) signal between 2000 cm^{-1} and 2300 cm^{-1}.[13] When coordination of the isocyanide towards a metal occurs via σ–donation of the lone pair of the carbon atom[1,3,13,14] a shift towards larger wavenumbers is observed in IR spectroscopy.[13] Such complexes generally show a linear geometry, preferred by metals such as gold, silver and copper.[3,12–14] The directed coordination properties of isocyanides result in a upright arrangement when deposited on a gold surface.[1,5,14] This feature is of particular interest for applications in the fields of sensing, surface functionalization, and molecular electronics, where the solid support acting as electrode is often a gold surface.[16–20] Functional groups inert towards different chemical environments and with high affinity to gold are required for surface functionalization and for the integration of functional molecules. The stability of the isocyanide towards physiological pH, water, thiols, alcohols, amines as well as basic conditions,[3,12,13,15] moves this functional group into the focus of interest. However, structures profiting from isocyanides as coordination sites for gold ions are scarce and we here report the synthesis and the investigation of the binding properties with gold(I) ions of a macrocyclic ligand structure functionalized with isocyanides as coordination sites.

The formation of diisocyanide gold(I) complexes was reported to be favored under high isocyanide concentrations.[12,13] An alternative strategy to increase the local isocyanide concentration might be the design of bidentate ligand structures, as sketched in Figure 1. We here present the macrocyclic ligand **1** with two isocyanide groups pointing inside and facing each other, with the intention to maintain a linear geometry for a coordinating metal ion as reported for bisphenylisocyanide gold(I) complexes.[9,21–24] As depicted in Figure 1, the target structure **1** was furthermore decorated with *tert*-butyl groups, which have a twofold role in the molecular design. First, they are expected to increase the compounds solubility and thus its processability in organic solvents. And second, their bulkiness pushes them to the periphery of the structure directing the isocyanides towards the center of the macrocycle. The expectation is that the high electron density in the center of the macrocycle becomes a favorable binding side for gold(I) cations, while the bulky periphery of the macrocyclic complex hinders the stacking triggered by aurophilic interactions.[21,25–28] We were thus eager to synthesize the macrocyclic ligand **1**, which should allow to obtain an individually dissolved and separated gold(I) complex upon coordination. Together with the synthesis of the macrocyclic

[a] C. Kress, D. Häussinger, P. Zwick, A. Prescimone, M. Mayor
Department of Chemistry, University of Basel, St. Johanns-Ring 19, 4056 Basel, Switzerland
E-mail: marcel.mayor@unibas.ch

[b] M. Mayor
Institute for Nanotechnology (INT), Karlsruhe Institute of Technology (KIT), P. O. Box 3640, 76021 Karlsruhe, Germany

[c] M. Mayor
Lehn Institute of Functional Materials (LIFM), School of Chemistry, Sun Yat-Sen University (SYSU), 510275 Guangzhou, China

Supporting information for this article is available on the WWW under https://doi.org/10.1002/ejic.202400408

Research Article
doi.org/10.1002/ejic.202400408

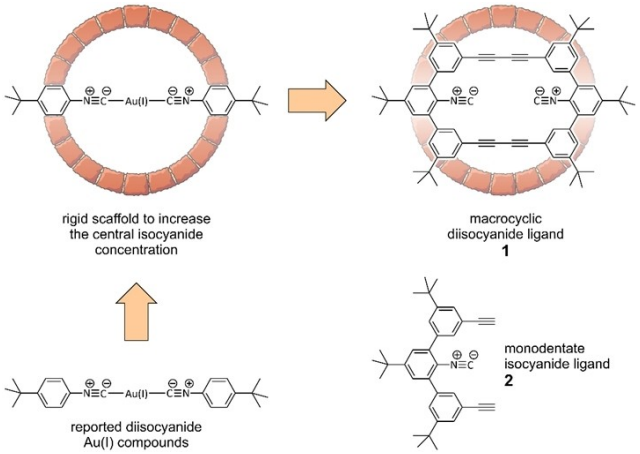

Figure 1. Concept to increase the local isocyanide concentration by macrocyclization. Representation of the rigid macrocyclic diisocyanide ligand **1** and the mono isocyanide derivative **2**.

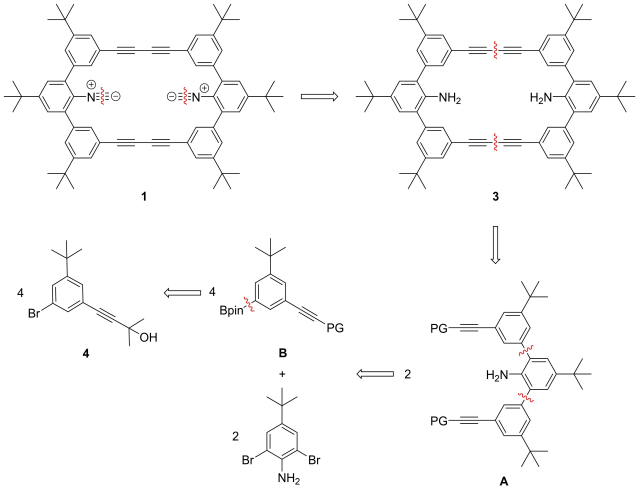

Scheme 1. Retrosynthesis of the macrocyclic ligand **1**.

ligand **1**, its complexation behavior with gold(I) ions is studied. The ligand and obtained complexes were analyzed by IR spectroscopy and UV–vis as well as NMR titration experiments and the bidentate ligand is compared to the monodentate model compound **2**, which can be considered as half of the macrocycle **1**.

Results and Discussion

Design and Retrosynthesis

The design of the ligand **1** is based on the idea to bridge two phenyl isocyanides to obtain a rigid macrocyclic bidentate ligand (see Figure 1). To allow for functionalization we envisioned to extend the central phenyl to a *meta*–terphenyl unit. The resulting symmetric structure can be decorated with functional groups allowing its dimerization. We envisioned to introduce 1,3–butadiynes as spacing units. As they are synthetically accessible via oxidative acetylene homocoupling, they serves as a natural breaking point in the retrosynthetic analysis of the macrocycle. To minimize the rotational degrees of freedom of the *meta*–terphenyl units and ensure an orientation of the isocyanides towards the inside of the macrocycle, the target structure was decorated with *tert*-butyl groups. The bulky substituents are further expected to enhance the solubility of **1** and to prevent aggregation of the gold complex either by π–π stacking or by aurophilic interactions.

As sketched in Scheme 1, the retrosynthetic analysis of the bidentate ligand **1** is straight forward. The isocyanides are introduced in the last step by treating the macrocyclic aniline **3**. The method of choice is based on the introduction of the formamide followed by water elimination.[2,13] An alternative radical approach[13] was not considered due to potential stability issues of the 1,3–butadiynes under these conditions. The 1,3–butadiyne subunits are accessible by oxidative acetylene homo coupling and ideally suited as retrosynthetic breaking points of the macrocyclization. The twofold coupling between identical functional groups not only reduces stoichiometry issues, but also results in the terphenyl precursor **A** of high symmetry. In order to favor dimerization of the bifunctional **A** to form the desired macrocycle over longer oligomerization products, high dilution conditions might be considered to favor the intramolecular ring closing over intermolecular chain elongations. The strategy was further motivated by our recent rather high yielding macrocyclizations of diethynyl precursors based on *Eglinton* and *Breslow* reaction conditions with copper(I) and copper(II) in pyridine under inert atmosphere.[29,30] The terphenyl precursor **A** should be accessible via a twofold *Suzuki Miyaura* cross coupling reaction between commercially available 2,6-dibromo-4-tertbutylaniline and **B**, which should be accessible by a *Myiaura* borylation of literature known **4**.[31]

The monodentate isocyanide ligand **2** should be accessible from the aniline precursor **A** applying similar transformations as discussed for the macrocycle **1**.

Synthesis and Characterization

The synthesis of **1** and **2** follows at large the retrosynthetic considerations, is displayed in Scheme 2, and discussed in details in the following. Literature reported **4**[31] was obtained in a yield of 70%. The polar acetylene protecting group was instrumental for the isolation of the desired product from the statistical *Sonogashira-Hagihara* cross coupling reaction mixture by silica gel (SiO_2) column chromatography. The *Myiaura* borylation to **5** proceeded in good yields of 88%, however, the dehalogenated side product rendered the separation by column chromatography on SiO_2 challenging, due to very comparable polarities. The terphenyl **6** was isolated in a yield of 75%, after optimization of the twofold *Suzuki* cross coupling reaction. The most successful catalytic system found was $Pd(amphos)_2Cl_2$ as catalyst with dimethoxy ethane and water as solvents. $NaHCO_3$ was used as weak base to prevent potential

Research Article
doi.org/10.1002/ejic.202400408

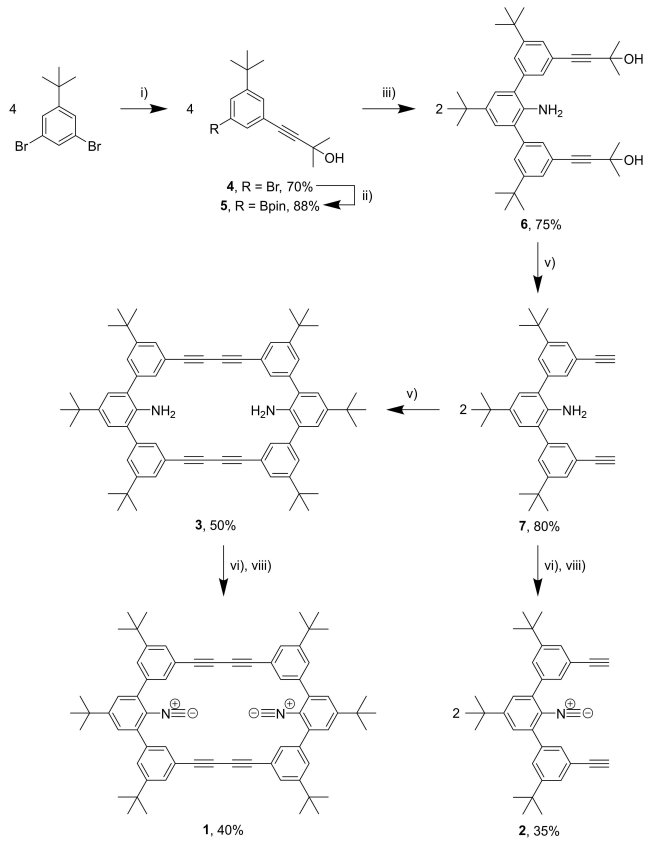

Scheme 2. Synthesis of the macrocyclic bidentate diisocyanide ligand **1** and the monoisocyanide derivative **2**. i) 2–methyl–3–butyne–2–ol, $Pd(PPh_3)_2Cl_2$, CuI, THF, Et_3N, 70 °C, 16 h, ii) $B_2(pin)_2$, KOAc, $PdCl_2(dppf)$, 1,4-dioxane, reflux, 2 h, iii) 2,5-dibromo-4-tertbutylaniline, $Pd(amphos)_2Cl_2$, $NaHCO_3$, DME, H_2O, 80 °C, 16 h, iv) KOH, Toluene, reflux, 3 h, v) $Cu(OAc)_2$, CuCl, pyridine (1.3 mM), 70 °C, 24 h, vi) HCOOH, $(Ac)_2O$, THF, rt, 2 h, vii) $POCl_3$, CH_2Cl_2, Et_3N, rt, 4 h.

elimination of the alcohol of the acetylene protecting group. Deprotection using potassium hydroxide yielded **7** in 80% yield. When sodium hydroxide was used instead, the reaction proceeded with lower yields. Macrocycle **3** was obtained after twofold acetylene homo coupling under *Eglinton* and *Breslow* conditions as pale white solid. Best yields of the macrocycle were obtained with a pseudo high dilution strategy. Large excesses of copper (I) chloride (18 equivalents) and copper (II) acetate (27 equivalents) were dissolved in dry pyridine, degassed and heated to 70 °C. The dialkyne **7** was also dissolved in pyridine (about one fourth of the volume of the reaction mixture) and degassed, before being added dropwise over 16 hours to the 70 °C hot and stirred reaction mixture. After completion of the addition, the theoretical maximal concentration of **7** would be 1.3 mM, which was never reached as the compound was continuously consumed. After work up of the reaction mixture, the macrocycle **3** was isolated by automated recycling gel permeation chromatography (GPC) in 50% yield. Besides the desired target **3**, larger macrocycles and open chain oligomers were observed as main side products. As final step, the two amine groups of **3** had to be transferred to isocyanides. Acetic formate was prepared by mixing acetic anhydride and formic acid in a two to one ratio and the mixture was allowed to cool down to room temperature after heating to 60 °C. The macrocycle **3** dissolved in THF was added and the course of the reaction was monitored by TLC. The crude diformamide intermediate was isolated and dehydrated with $POCl_3$ in a mixture of CH_2Cl_2 and triethylamine. The desired isocyanide macrocycle **1** was isolated in 40% yield as a white solid after work up and SiO_2 column chromatography.

Half the macrocycle as monodentate model compound **2** was obtained in a similar two step procedure. The amine **7** was treated with acetic formate to obtain the intermediate formamide, which was isolated as crude and treated with $POCl_3$ to provide the isocyanide **2** as white solid in 35% yield after SiO_2 column chromatography.

The identities of the new structures were corroborated by high-resolution electrospray ionization mass spectrometry (HRMS), proton nuclear magnetic resonance (^{1}H-NMR) and proton-decoupled carbon NMR ($^{13}C\{^1H\}$–NMR) spectroscopy. The ligands **1** and **2** were furthermore characterized by IR and UV-vis spectroscopy, while the solid-state structure of **1** was elucidated by single crystal x-ray crystallography. Detailed experimental procedures and all analytical data can be found in the supporting information (SI). The full characterization of **7**, **3**, **2** and **1** was performed by state-of-the-art NMR spectroscopy. Characteristic shifts for the aromatic hydrogen atoms were recorded as displayed in Figure 2. For the purple labeled proton, a significant downfield shift of 0.46 ppm can be observed upon macrocyclization of **7** to **3**. This shift can be attributed to the rigidity of the macrocycle which hinders the rotation of the outer phenyls of the *meta*-terphenyl unit. As expected in the ^{1}H–NMR spectrum, the acetylene signal vanishes upon homocoupling of **7** to **3** (see Figure SI-1 of the SI). The formation of the isocyanide leads to a downfield shift of 0.25 ppm for the orange labeled proton for the ligands **1** and **2**. Otherwise, only minor shift changes in the aromatic region can be observed upon formation of the isocyanides. The aniline signals reported for **7** and **3** vanish upon formation of the isocyanide (see Figure SI-1 of the SI). The free acetylene of **7** was found to be stable towards the formation of the isocyanide **2** and its chemical shift in the ^{1}H-NMR remains almost the same.

The Isocyanide ligands **1** and **2** were furthermore characterized by IR and UV-vis spectroscopy. Their spectra are displayed as starting points of the corresponding titration experiments in Figure 3 for IR-experiments and in Figure 5 for UV-vis investigations (further spectra are provided in the SI).

The IR spectra of both, **1** and **2** display a sharp peak at 2100 cm^{-1}, characteristic for free isocyanides with full triple bond character (labeled by a green background in Figure 3).[1,13,14] Also the signal attributed to the free acetylene at 3300 cm^{-1} can clearly be observed for **2**.

The UV-vis spectra of both derivatives (Figure SI-2) show a broad peak at 240 nm with an extinction coefficient varying by a factor of two. The peak can be attributed to the *meta*–therphenyl unit as reported in literature.[32] This absorption peak furthermore suggests, that the two *meta*–therphenyl units of **1** act independently from each other and are not conjugated as expected for a *meta* substitution pattern.[33] The macrocycle **1** shows three more peaks with maxima at 296 nm, 314 nm and

Research Article
doi.org/10.1002/ejic.202400408

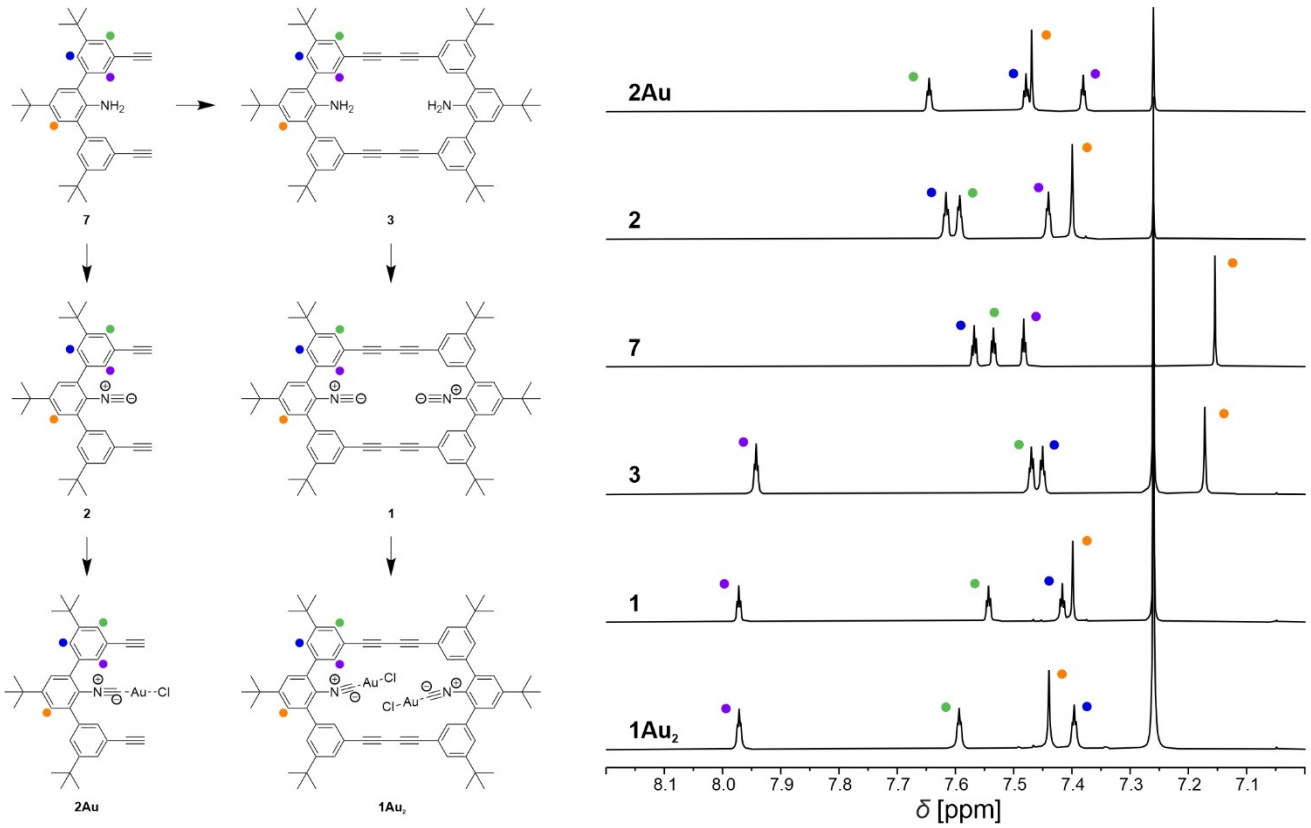

Figure 2. ^{1}H–NMR spectra (500 MHz, $CDCl_3$, 298 K) of the macrocyclization precursor **7**, the macrocycle **3**, the isocyanide ligands **1** and **2** and the gold(I) complexes **1Au$_2$** and **2Au**. The assignment of the signals is indicated by colored dots.

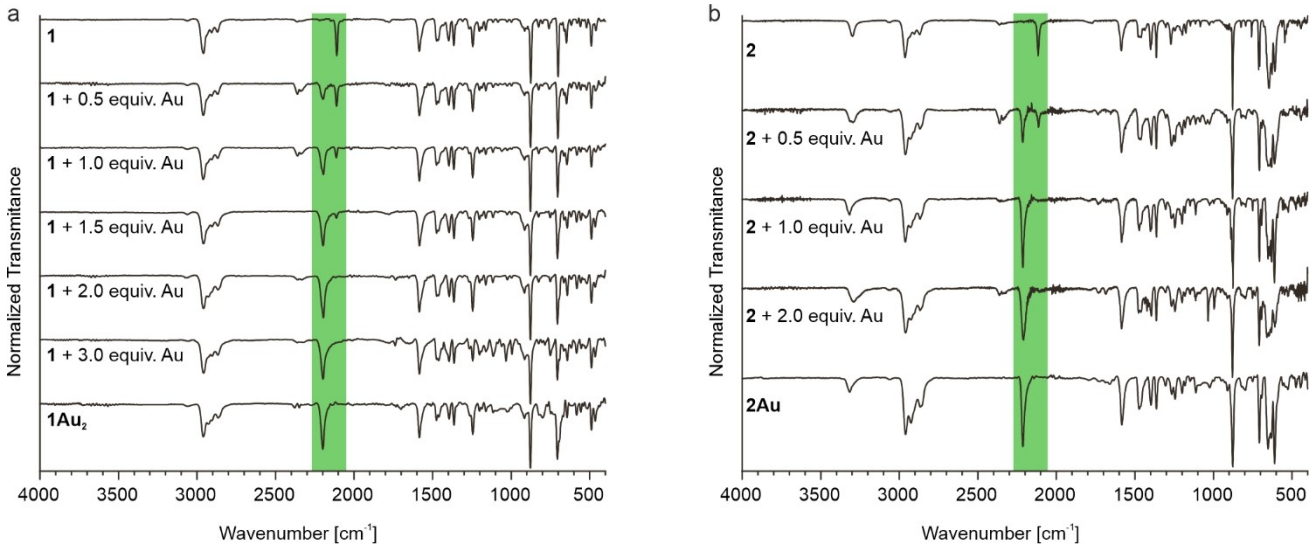

Figure 3. IR spectra of the ligands **1** (a) and **2** (b) and of the complexes **1Au$_2$** (a) and **2Au** (b) including a titration of **1** (a) and **2** (b) with $Au[S(CH_3)_2]Cl$. The spectra of the IR titration were recorded after the addition of the indicated amount of $Au[S(CH_3)_2]Cl$ salt to the ligands **1** and **2**. The green label covers the frequencies with the isocyanide signals.

333 nm. These peaks were attributed to the 1,4-diphenyl-1,3-butadiyne spacer in analogy to literature compounds.[30] Furthermore, this is the only structural difference between **1** and **2**.

Complexation and Coordination Stoichiometry

The first complexation experiments of **1** and **2** with different amounts of $Au[S(CH_3)_2]Cl$ as gold(I) source were analyze by IR spectroscopy and are summarized in Figure 3. Upon addition of

Research Article
doi.org/10.1002/ejic.202400408

gold salt a sharp new signal at 2200 cm^{-1} (see green label), characteristic for the isocyanide coordinating to the gold atom with triple bond character,[1,14] arises. Besides this characteristic peak no other significant changes were observed, indicating, that the 1,3–butadiynes as well as the free acetylene (see peak at 3300 cm^{-1}) seem to be inert towards the used gold source. This allows to conclude, that the ligands do not undergo undesired side reactions under the applied complexation conditions and that the observed spectroscopic changes arise from the coordination of the isocyanide towards gold. The unexpected signals occasionally observed between 2300 cm^{-1} and 2400 cm^{-1} arise from CO_2 impurities in the samples and don't belong to the investigated compounds.[34,35]

A closer inspection of the IR spectra during the titration of **1** gave first indications of the system's stoichiometry. As already mentioned above, a second peak at 2200 cm^{-1} appears with the addition of $Au[S(CH_3)_2]Cl$. This peak becomes more dominant when more salt is added and after the addition of two equivalents (equiv.), it is the only remaining signal. Further addition of gold salt does no longer alter the IR spectra. It thus seems that exclusively signals for the free isocyanide group (2100 cm^{-1}) and for the isocyanide group coordinating an Au(I) ion (2200 cm^{-1}) are observed. The ratio between the signal intensities is not quantitative but a clear trend of the prevalent species can be observed. The saturation of the macrocyclic ligand **1** with two equiv. of Au(I) salt clearly suggests a 1 : 2 stoichiometry, with both isocyanides coordinating one gold(I) ion each, resulting in a **1Au$_2$** complex. Similar IR titration experiments were performed with other sources of Au(I) ions (JohnPhos $Au(MeCN)SbF_6$, see Figure SI-3a of the SI), showing comparable results, namely the formation of **1Au$_2$**. Also the IR titration of **2** with 0.5, 1.0, and 2.0 equiv. of $Au[S(CH_3)_2]Cl$ salt showed exclusively either the free or coordinated isocyanide. For ligand **2**, the saturation was reached with 1.0 equiv. of gold(I) salt added, pointing at the expected 1 : 1 stoichiometry and the formation of the **2Au** complex. Again, the result was independent from the used Au(I) source (Figure SI-3b of the SI).

Based on the determined stoichiometry the complexes **1Au$_2$** and **2Au** were synthesized by treating the ligands **1** and **2** with $Au[S(CH_3)_2]Cl$ in chloroform. The complexes **1Au$_2$** and **2Au** were isolated as white solids in excellent yields of 78% and quantitative, respectively. The IR spectra of the complexes **1Au$_2$** and **2Au** resemble the ones of **1** and **2** after the addition of 2.0 and 1.0 equiv. of Au(I) salt respectively, and corroborate the stoichiometry determined by the titration experiments. The Au(I) complexes **1Au$_2$** and **2Au** were fully characterized by HRMS, ^{1}H-NMR, $^{13}C\{^1H\}$–NMR and UV-vis spectroscopy (see SI). The aromatic regions of the ^{1}H-NMR spectra of **1Au$_2$** and **2Au** are displayed in Figure 2. The signal multiplicities and moderate shift changes upon complexation point at only minor alterations of the ligands' structures and that their high symmetry is maintained.

The blue and green labeled protons in Figure 2 show the same spectroscopic trends upon complexation for the two ligands. For the orange labeled proton, instead, a significant common down field shift was recorded. For **1Au$_2$**, the only proton with unchanged signal is the purple labeled one facing towards the isocyanide. Interestingly, for **2Au** this proton is significantly up field shifted. Generally, the shift changes observed for **2Au** are slightly stronger than the ones of **1Au$_2$** compared to the ligands **2** and **1**, respectively. Furthermore, the signals of **2Au**, compared to the ones of **2**, show trends towards the macrocyclic structures **1** and **1Au$_2$** for the blue and green protons. This indicates that the flexibility of the monoisocyanide ligand **2** decreases upon complexation.

The structures of **1** and **1Au$_2$** were further corroborated by x-ray crystallography (Figure 4). Single crystals of the macrocycle **1** were obtained by slow diffusion of methanol into a solution of **1** in chloroform. The lamellar packing of the crystal structure of **1** shows the formation of a tubular arrangement

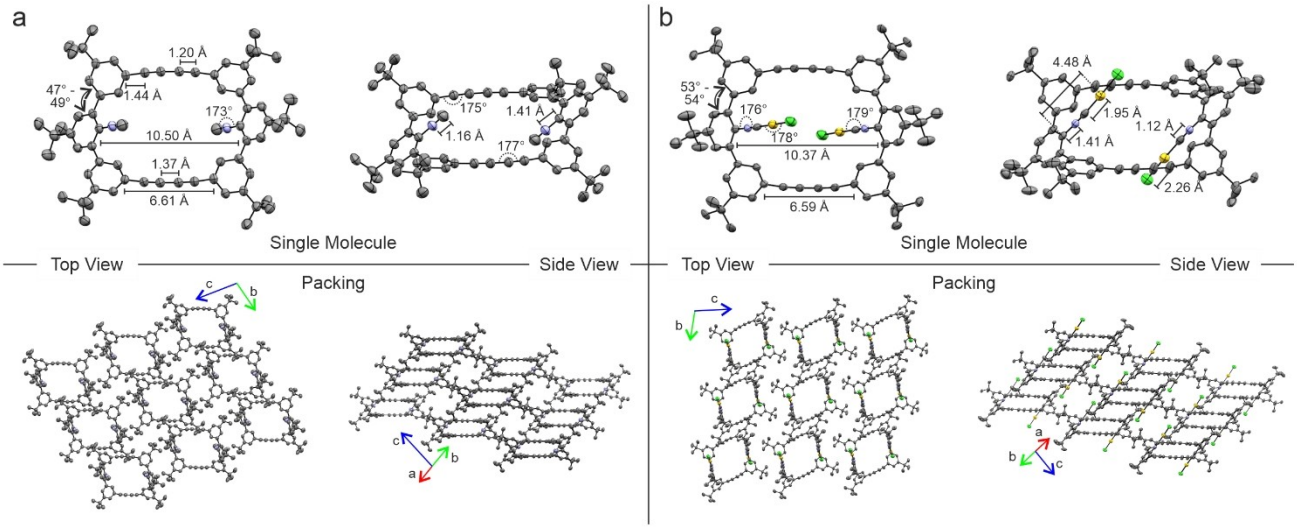

Figure 4. Solid state structure of the diisocyanide ligand **1** (a) and of the complex **1Au$_2$** (b). The single molecules are shown on top with different orientations. For both structures the unit cell includes two molecules. The lamellar type crystal packing forms tubes filled with solvent molecules. The Oak Ridge Thermal Ellipsoid Plots (ORTEP) are plotted on a 50% probability. The hydrogen atoms and solvent molecules (chloroform and heptane) are omitted for clarity.

(best visible in the top view of Figure 4a). From the side view, parallel planes arising from the linear 1,3–butadiynes are interlocked diagonally by the phenyl-isocyanide subunits. The two isocyanide functional groups are facing towards the cavity of the macrocyclic structure while pointing out of the plane into opposed directions. The spatial arrangement of the isocyanides results from the saddle shape of the molecule. The *meta*–terphenyl units are not planar due to steric clashes of the aromatic protons, leading to a dihedral angle between 47° and 49°. The cavity has a length of 10.50 Å while the 1,3-butadiynes measure 6.61 Å with a clear alternating bond length, confirming the presence of the triple bonds. The angles of 175° and 177° within the spacing unit are comparable to each other and show that the 1,3–buatadiynes are not significantly strained. The isocyanides are almost linear with an angle of 173°.[3,12–15] The bond length of 1.16 Å is furthermore in good agreement with literature reports.[3,12–15] Overall, the crystal structure and IR spectroscopy confirm the triple bond character of the free isocyanide with a lone pair on the carbon atom able to undergo σ-donor coordination to a metal.[1,3,13]

Single crystals of **1Au$_2$** were obtained by slow diffusion of heptane into a chloroform solution of the compound. The solid-state structure of **1Au$_2$** is displayed in Figure 4b and shows the presence of two gold atoms coordinating in a linear fashion to the isocyanides. The charge of the coordinated Au(I) cations is compensated by chloride anions on the opposed side. The linearity of the arrangement is confirmed by the angles ranging from 176° to 179° for the entire coordination sphere. The isocyanide length of 1.12 Å and its bond to the phenyl of 1.41 Å are comparable to those of **1**. The carbon to gold bond of 1.95 Å is significantly longer, while the chlorine counter ion is even further apart. The angles as well as bond lengths resulting from the crystal structure are comparable to the literature reports of bisphenylisocyanide gold(I).[23,36] Overall, the size of the cavity seems to shrink upon complexation, resulting in a length of 10.37 Å while the 1,3–butadiynes measure 6.59 Å. From the side views, an increase in dihedral angle within the *meta*–terphenyl units reaching 53° to 54° can be observed. The lamellar packing as well as tubular arrangement of **1Au$_2$** is similar to that of **1**.

Gold in the oxidation state one generally undergoes intermolecular gold-to-gold interactions with hydrogen bonding-like strength called aurophilicity.[25,37,38] While rather weak aurophilic bonds are generally observed for gold(I) to isocyanide complexes,[25] our crystal structure does not indicate such type of interactions. The intramolecular linear moieties are well separated from each other with an intramolecular Au–Au distance of 8.34 Å and an intermolecular distance of 6.86 Å. The coordination spheres within a molecule are facing towards the cavity filled with solvent molecules (heptane). Intermolecular gold-to-gold interactions are not possible due to the packing of the crystal structure, which is controlled by a variety of parameters including among others chloroform molecules, the steric requirements of the *tert*-butyl groups, and the rigidity of the ligand **1**.

The 1:2 stoichiometry of the ligand **1** with the gold salt Au[S(CH$_3$)$_2$]Cl was furthermore confirmed by the method of continuous variation via UV-vis experiments as reported in Figure SI-4 of the SI. The plot shows a clear sharp maximum at a molar fraction of 0.68. The rather angular than parabolic shape of the plot indicates a high association of the isocyanide towards gold.[39] It is known, that the method of continues variation is not ideally suited to determine the stoichiometry of a host guest system, in particular of higher order.[40,41] However, in the here reported case it confirms the stoichiometry deduced from the IR-titration experiments. With the knowledge concerning the stoichiometry, the focus was set on the determination of the association constants (K_a) involved in the system.

Estimation of the Association Constants

The first titration experiments were performed with **2** and UV-vis spectroscopy was considered as method of choice. The UV-vis spectra were recorded at concentrations of 3.04 μM in 1,2–dichloroethane at 20 °C with the intention to obtain a nonlinear region when plotting the difference in absorption against the concentration of added guest (Au[S(CH$_3$)$_2$]Cl). A curved region with binding probabilities (p) in the range of $0.2 < p < 0.8$ (with $p = [HG]/[G]_0$ for $[H]_0 \geq [G]_0$ and $p = [HG]/[H]_0$ for $[H]_0 < [G]_0$) is required to determine the K_a of the system.[40,41] Au[S(CH$_3$)$_2$]Cl was chosen as guest as it is almost silent in the UV region of interest, with a low extinction coefficient between 220 nm and 255 nm (see Figure SI-2). The UV-vis titration experiment of **2** with Au[S(CH$_3$)$_2$]Cl is shown in Figure 5a. A clear increase in absorption can be observed between 260 nm and 330 nm upon addition of Au(I) ions, while two new shoulders arise at 250 nm and 230 nm. The change in absorption between 260 nm and 330 nm can be observed only until the addition of one equiv. of guest. At the maximum of the ligand of 241 nm, an initial decrease in absorption can be observed upon addition of guest. This leads to the formation of isosbestic points at 233 nm and 245 nm, indicating a 1:1 system.[40,41] Upon addition of more than one equiv. of Au(I) ions, only a continuous increase between 220 nm and 255 nm was observed, arising from the absorption properties of the guest. The plots of the difference in absorption *vs.* the amount of added guest at 310 nm, 285 nm and 280 nm display basically two linear regions (Figure 5b), pointing at a high affinity of the host guest system. The plot is characteristic for an immediately saturated system and only a very few data points in the curved region around 1 equiv. of Au[S(CH$_3$)$_2$]Cl could be collected. The binding probability (p) seems to be 1 and thus the system is outside the region where reliable K_a values can be determined. The data was nevertheless processed with the intention to estimate an association constant and a K_a value of $3.0 \cdot 10^8$ M^{-1} (SSR = $6.9 \cdot 10^{-6}$) was obtained. The value was obtained by the determination of only one parameter for each wavelength (the difference in extinction coefficient between the two species, $\varepsilon_{\Delta(HG\text{-}H)}(310\text{ nm}) = 3975$, $\varepsilon_{\Delta(HG\text{-}H)}(285\text{ nm}) = 8549$, $\varepsilon_{\Delta(HG\text{-}H)}(280\text{ nm}) = 8969$, see summary in Figure SI–5). The resulting differences in absorption coefficients are in agreement with the results obtained from the UV–vis spectra of the isolated ligand **2** and its complex **2Au**. A similar K_a value of $2.4 \cdot 10^8$ M^{-1} (SSR = $9.0 \cdot 10^{-6}$) was obtained when using

Research Article
doi.org/10.1002/ejic.202400408

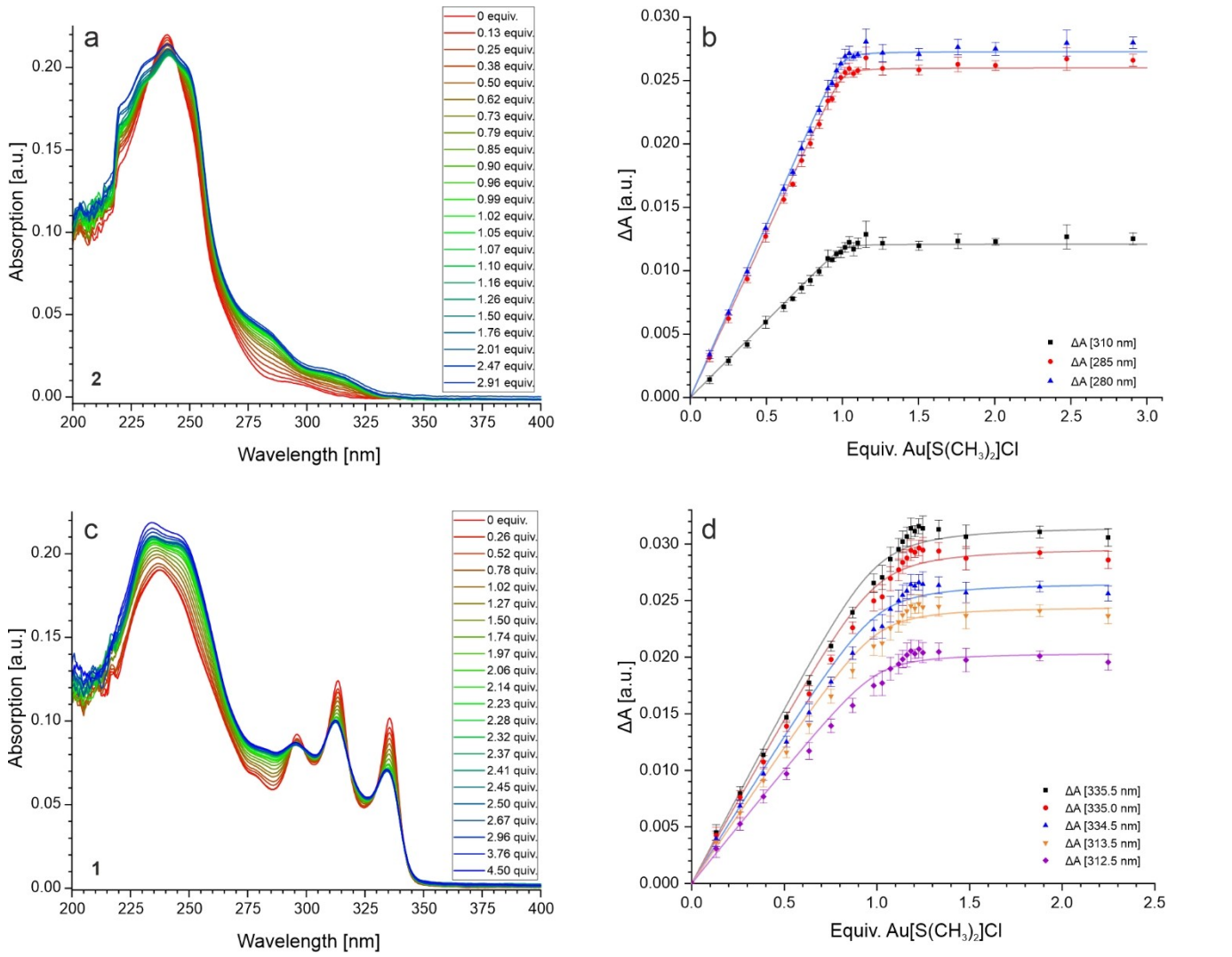

Figure 5. Absorption spectra and result of the UV-vis titration experiment of the ligand **2** (a) and **1** (c) with the addition of $Au[S(CH_3)_2]Cl$, measurement in 1,2–dichloroethane, 20 °C, at concentrations of 3.04 μM for **2** and 1.52 μM for **1**. On the right side (b and d respectively) the difference in absorption is plotted against the equiv. of $Au[S(CH_3)_2]Cl$ salt added. It is important to note, that the concentration of the $Au[S(CH_3)_2]Cl$ salt is divided by a factor of two for graph d. The filled symbols show the experimental values with error ranges obtained from statistics. The solid lines correspond to the simulated values obtained with the K_a and ε_Δ values determined with the UV-vis titration experiment.

the calculator Bindfit,[41] which required a total of 7 parameters for the three wavelengths including the three extinction coefficients (see summary in Figure SI-5). Both methods, relying on non-linear regressions, allowed to independently determine comparable and extremely high association constants. The obtained values for the extinction coefficients are comparable to each other. A common method to judge the quality of high association constants is to determine the $[H]_0/K_d$ ratio of the system (with $K_d = 1/K_a$), with the rule of thumb that for systems with $[H]_0/K_d > 100$ the titration experiments contain only little information but still allow to determine a reasonable K_a for simple 1:1 systems, while for a ratio of $[H]_0/K_d > 1000$ the obtained information is restricted to a level, that no reliable results can be obtained anymore.[41] Generally, when employing a global analysis approach, association constants can be determined until $[H]_0/K_d \approx 100$.[41] Beyond this value, only estimations of the K_a can be obtained.[41] Inspecting the UV-vis titration experiment of **2** with $Au[S(CH_3)_2]Cl$ gives a ratio $[H]_0/K_d = 900$, such that the obtained $K_a = 3.0 \cdot 10^8\ M^{-1}$ cannot be considered as reliable value. In order to obtain more reliable values for K_a, methods enabling the detection of lower concentration of $[H]_0$ would be required.

The UV-vis titration experiment of **1** with $Au[S(CH_3)_2]Cl$ is displayed in Figure 5c. For **1**, an increase in absorption can be observed upon complexation for the maximum at 238 nm with two shoulders arising. Significant changes can be observed until the addition of about 2.0 equiv. to 2.5 equiv. of guest, while changes upon further additions can be attributed to the absorption of the Au(I) salt itself (see UV-vis spectrum in Figure SI-2 of the SI) and slow evaporation of the solvent. In the region between 260 nm and 350 nm generally an increase in absorption can be observed for the minima, while a decrease results for the maxima. The changes in absorption are observable until the addition of 2.0 equiv. to 2.5 equiv. of

Research Article
doi.org/10.1002/ejic.202400408

Au[S(CH_3)$_2$]Cl, which is in agreement with our expectation based on the stoichiometry of the system. The linear changes in absorption result unexpectedly in the formation of isosbestic points, usually observed for 1:1 systems. The presence of isosbestic points means that only two different species can be differentiated. Most likely, the macrocycle consists of two independent coordination sites for Au(I) ions and the coordination of the first Au(I) ion causes very comparable differences in the absorption spectrum as the second one ($\varepsilon_{\Delta(HG-H)} \approx \varepsilon_{\Delta(HG2-HG)}$). In such a case the individual binding events leading to **1Au** and **1Au$_2$**, respectively, cannot be distinguished from each other in the UV-vis titration experiment, and instead an independent binding behavior of each isocyanide group towards a single gold(I) atom is postulated. In other words, instead of stepwise resolved association constants K_{a1} and K_{a2}, for the first and second binding event of a gold(I) atom to the macrocycle **1**, a single association constant K_a for the individual isocyanide group of **1** independently binding a gold(I) atom can be determined. This simplification of the system, based on the experimental results of the UV-vis titration, allows to treat the binding behavior of the macrocycle **1** as a 1:1 system. In order to arrange with the stoichiometry involved, the concentration of the Au[S(CH_3)$_2$]Cl salt used for the calculation was half of the real concentration, while the concentration of the macrocycle remained 1.52 μM. The in this way approximated K_a was $5.1{\cdot}10^7$ M^{-1} (SSR = $8.1{\cdot}10^{-5}$) (the difference in extinction coefficient are reported in Figure SI-6). Using Bindfit,[41] a comparable K_a value of $4.9{\cdot}10^7$ M^{-1} (SSR = $8.1{\cdot}10^{-5}$) was obtained (see summary in Figure SI–6). The estimation of the association constant is about 5 to 6 times smaller than the one approximated for **2**. Also a poorer fit between simulated and measured data is observed compared to the case of **2**, as the sum of squared errors increased by an order of magnitude (solid lines *vs.* data points in Figure 5b and d respectively). This is not solely due to the simplified "pseudo 1:1" treatment of the ligand **1**, as the previously introduced $[H]_0/K_d$ ratio as indicator of the reliability of the titration is with 70–80 a borderline case for a 1:1 system.

Overall, the analysis of association constants by UV-vis titration experiments turned out to be challenging, providing at best estimated values of limited reliability, given by the concentration of the ligands. As alternative approach fluorescence spectroscopy was considered, but discarded due to the poor signal and photodegradation of the macrocycle **1**. As further alternative providing more insights into the various structures formed during the titration experiment, NMR investigations were considered.

The ^{1}H-NMR titration experiment of **1** with Au[S(CH_3)$_2$]Cl in deuterated chloroform at 25 °C is depicted in Figure 6. The most downfield shifted proton at δ = 7.97 ppm (labeled in purple in Figure 2) splits in two equally intense resonances at 7.80 and 8.07 ppm, indicating the formation of an asymmetric mono-metalated 1:1 species (HG), **1Au** at first sight. Closer inspection by means of ^{1}H-^{13}C-HSQC spectra revealed, however, that even at 0.5 equiv. of Au[S(CH_3)$_2$]Cl a third species is also formed, that was attributed to the bis-metalated complex (HG_2), **1Au$_2$** (see Figure SI-7 of the SI). Unfortunately, the proton chemical shift of **1Au$_2$** is accidentally identical to that of **1** further increasing the complexity of the analysis. Fortunately, the shift of the corresponding carbon atom is with 132.55 ppm for **1Au$_2$** significantly up field shifted compared with the carbon resonance of **1** at 133.17 ppm. The intermediate mono-gold species **1Au** shows consequently two different carbon resonances at 132.17 and 133.51 ppm. On adding further equivalents of Au[S(CH_3)$_2$]Cl a small intensity increase of the resonances of **1Au** at 1.0 equiv. was observed but further titration showed a sharp decrease at 1.5 equiv. and complete disappearance at 2.0 equiv. and above, thus corroborating the 1:2 stoichiometry. Volume integration of the three species in the HSQC spectra allowed to quantify the equilibrium concentrations of the three species in the titration experiment and yielded the relative equilibrium constants:

$$K_2 = \frac{K_{a1}\,[HG_2][H]}{[HG]^2}$$

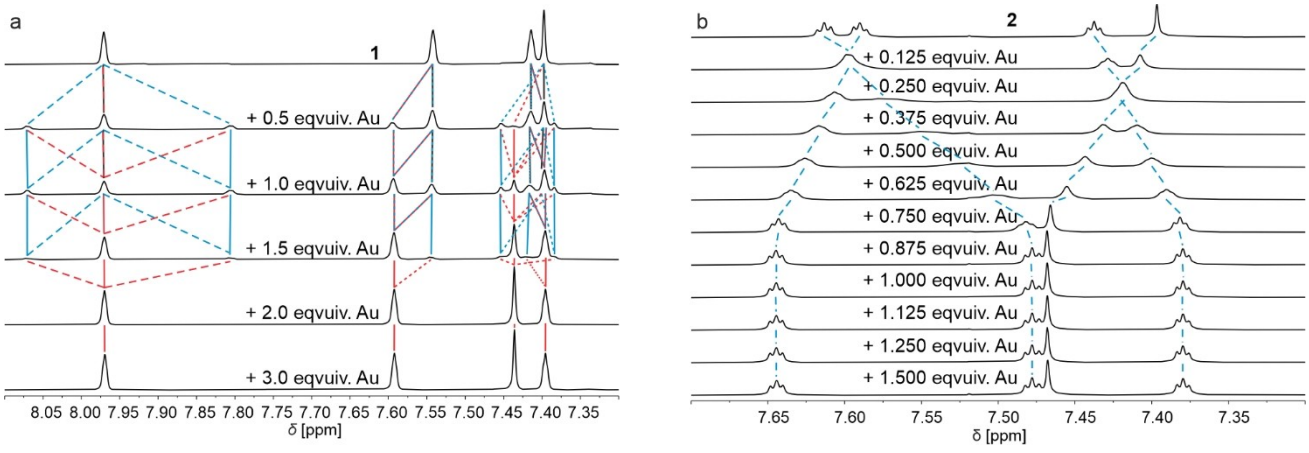

Figure 6. ^{1}H-NMR titration experiments of **1** (a) and **2** (b) with Au[S(CH_3)$_2$]Cl. The experiments were carried out in deuterated chloroform at 25 °C. The spectra of **1** were recorded on a 600 Hz spectrometer equipped with a very sensitive helium cooled cryogenic probe at a concentration of 1.53 mM. The spectra of **2** are recoded on a 400 Hz spectrometer with a concentration of 3.06 mM.

Research Article
doi.org/10.1002/ejic.202400408

$$\text{or}: \ \alpha = \frac{4 \times K_{a2}}{K_{a1}} = \frac{4 \ \times \ [HG_2][H]}{[HG]^2} = 1.96$$

The value of 1.96 for the cooperativity coefficient α indicates moderately positive cooperativity for the binding of the second Au(I) ion. However, in the solid-state structure of **1Au$_2$** (Figure 4b) intramolecular aurophilic interactions between both gold atoms were not observed and most likely, they are also absent in solution. Our hypothesis is thus that the coordination of the first Au(I) ion swivels out the second isocyanide group on the other side of the macrocycle's plane and makes it thereby better accessible for the coordination of the second Au(I) ion.

Interestingly, titration of **1** with Au[S(CH$_3$)$_2$]Cl reveals kinetics that are in the slow time regime for protons at 600 MHz. Therefore, EXSY exchange spectra were also recorded to get more insight into the kinetics of the system (see Figure SI-8 of the SI). While a complete analysis was hampered by the accidental overlap of the ^{1}H resonances of **1** and **1Au$_2$**, it was possible to extract an approximate k_{off} rate for **1Au$_2$** from the volume integrals of the titration point with 1.5 equiv. of Au[S(CH$_3$)$_2$]Cl, where the molar fraction of the free host **1** is negligible (<2%). Analysis according to Equation (29) by C. L. Perrin and T. J. Dwyer[42] for the non-symmetric two site exchange yielded a k_{off} rate for **1Au$_2$** of 0.20 s^{-1}. Assuming a diffusion controlled k_{on} rate of $1x10^8$ $M^{-1}s^{-1}$ an equilibrium constant K_{a2} of $5.0{\cdot}10^8$ M^{-1} was obtained (see summary in Figure SI-9 of the SI). With the relation from the HSQC experiments a K_{a1} of $2.5{\cdot}10^8$ M^{-1} can be postulated. The K_a values estimated from the NMR-titration experiments for **1** are about one order of magnitude larger than the lower boundary extracted from the UV-Vis titration experiments. Thus, both results agree with each other. It is however worth mentioning that both titrations were not performed in the same solvent which hampers the direct comparison.

In contrast to the slow exchange time regime observed for the NMR titration of **1**, a similar titration of **2** with Au[S(CH$_3$)$_2$]Cl showed progressive changes of the chemical shifts of the aromatic protons (Figure 6b). The line shape observed at 3.06 mM concentration and 400 MHz indicates an intermediate to fast exchange regime on the NMR time scale in the order of several 10 s^{-1}.[43] Assuming again a diffusion controlled k_{on} rate of $1x10^8$ $M^{-1}s^{-1}$, an equilibrium constant K_a in between $5{\cdot}10^6$ M^{-1} and $1{\cdot}10^7$ M^{-1} is obtained. Even so the estimation of the K_a value by NMR experiments has been done in a different solvent ($CDCl_3$), the value is more reliable than the one obtained above by UV-vis titration (measured in 1,2-dichloroethane).

The estimations extracted from the NMR titration experiments suggest one order of magnitude larger association constants for the macrocycle **1** compared with half cycle model compound **2**. This larger affinity of **1** to Au(I) ions may be rationalized with the increased concentration of negative charge in the macrocycles center induced by both isocyanide groups.

Conclusions

The macrocyclic diisocyanide ligand **1** and half of the structure, the isocyanide ligand **2** and the corresponding gold(I) complexes **1Au$_2$** and **2Au** were synthesized and characterized. The stoichiometry of the systems were analyzed displaying that each isocyanide coordinates to one Au(I) ion. The coordination takes place in a linear fashion and the triple bond character of the isocyanide is preserved. Neither the free acetylene of **2** nor the 1,3-butadiynes of **1** interact with the coordinated gold ion. Potentially possible aurophilic interactions were neither observed in the solid-state structure of **1Au$_2$** nor in NMR experiments.

Titration experiments to determine the isocyanides affinity to Au(I) ions turned out to be challenging, as none of the analytical methods allowed to work with samples of the required dilution, as fluorescence experiments turned out to be impossible due to limitation in the photostability of the ligand structures. While UV–vis based titrations analyzing the thermodynamics of the system allowed to estimate threshold values of the association constant, kinetic values extracted from NMR experiments provided further insights. The K_{a2} of **1Au** to **1Au$_2$** was estimated to be $5.0{\cdot}10^8$ M^{-1}, by assuming a diffusion controlled k_{on} rate of $1x10^8$ $M^{-1}s^{-1}$. The obtained value, combined with the thermodynamically determined cooperativity of 1.96, allowed to obtain a value of K_{a1} of $2.5{\cdot}10^8$ M^{-1} for **1** to **1Au**. The complexation of monodentate isocyanide ligand **2** to **2Au** revealed a slightly lower association constant, pointing at the missing cooperativity and the higher flexibility of the system.

To the best of our knowledge, this is one of the first attempts to quantify the interaction between isocyanides and Au(I) ions, even so the obtained data rather provide boundary values and pretty accurate estimations. The study further documents both, affinity and directionality of the isocyanide Au(I) interaction, which might be interesting aspects for potential applications.

The intention, the coordination of a Au(I) ion by an intramolecular pair of isocyanides, was not observed for the here reported macrocyclic ligand **1**. Most likely the rigid scaffold of the macrocycle does not allow to adjust the spacing of the isocyanides, such that the coordination of a pair of gold ions is favored. Our current attempts towards diisocyanide ligands forming 1:1 complexes with gold (I) ions are thus based on scaffolds with either reduced distance between both isocyanide groups or with increased flexibility.

Supporting Information Summary

The Supporting Information comprises: additional figures cited in the text (Figures of the Supporting Information), general remarks, a synthesis overview, the experimental procedures and characterization and crystallographic data. Deposition Numbers 2297114 (**1**) and 2297113 (**1Au$_2$**) contain the supplementary crystallographic data for this paper. These data are provided free of charge by the joint Cambridge Crystallographic Data

Centre and Fachinformationszentrum Karlsruhe Access Structures service. The authors have cited references within the Supporting Information.[31]

Acknowledgements

The Mayor group acknowledges generous support by the Swiss National Science Foundation (200020_207744). M.M. acknowledges support from the 111 project (Grant No. 90002–18011002). Open Access funding provided by Universität Basel.

Conflict of Interests

The authors declare no conflict of interest.

Data Availability Statement

The data that support the findings of this study are available in the supplementary material of this article.

Keywords: Isocyanide ligands · Gold · Host-guest systems · Macrocyclic ligands · Aurophilicity

[1] M. V. Barybin, J. J. Meyers Jr, B. M. Neal, in *Isocyanide Chemistry*, (Eds.: V. G. Nenajdenko), John Wiley & Sons, Ltd **2012**, pp. 493–529.
[2] N. Liu, F. Chao, M.-G. Liu, N.-Y. Huang, K. Zou, L. Wang, *J. Org. Chem.* **2019**, *84*, 2366–2371.
[3] A. Massarotti, F. Brunelli, S. Aprile, M. Giustiniano, G. C. Tron, *Chem. Rev.* **2021**, *121*, 10742–10788.
[4] R. Abuflaha, D. Olson, D. W. Bennett, W. T. Tysoe, *Surf. Sci.* **2016**, *649*, 56–59.
[5] M. Garvey, J. Kestell, R. Abuflaha, D. W. Bennett, G. Henkelman, W. T. Tysoe, *J. Phys. Chem. C* **2014**, *118*, 20899–20907.
[6] P. Herr, C. Kerzig, C. B. Larsen, D. Häussinger, O. S. Wenger, *Nat. Chem.* **2021**, *13*, 956–962.
[7] P. Herr, A. Schwab, S. Kupfer, O. S. Wenger, *ChemPhotoChem* **2022**, *6*, e202200052.
[8] T. Ogawa, N. Sinha, B. Pfund, A. Prescimone, O. S. Wenger, *J. Am. Chem. Soc.* **2022**, *144*, 21948–21960.
[9] A. Vladyka, M. L. Perrin, J. Overbeck, R. R. Ferradás, V. García-Suárez, M. Gantenbein, J. Brunner, M. Mayor, J. Ferrer, M. Calame, *Nat. Commun.* **2019**, *10*, 1–9.
[10] E. Lörtscher, C. J. Cho, M. Mayor, M. Tschudy, C. Rettner, H. Riel, *ChemPhysChem* **2011**, *12*, 1677–1682.
[11] M. Kiguchi, S. Miura, K. Hara, M. Sawamura, K. Murakoshi, *Appl. Phys. Lett.* **2006**, *89*, 213104.
[12] L. Malatesta, in *Progress in Inorganic Chemistry*, (Eds.: F. A. Cotton), John Wiley & Sons, Ltd **1959**, pp. 283–379.
[13] J. A. Green, P. T. Hoffmann and P. Hoffmann, G. Gokel, D. Marquarding, I. Ugi, in *Isonitrile Chemistry*, (Eds.: I. Ugi), Elsevier, **2012**, pp. 1–64.
[14] M. Lazar, R. J. Angelici, in *Modern Surface Organometallic Chemistry*, (Eds.: J.-M. Basset, R. Psaro, D. Roberto, R. Ugo), John Wiley & Sons, Ltd **2009**, pp. 513–556.
[15] M. A. Mironov, *Isocyanide Chemistry*, John Wiley & Sons, Ltd, **2012**, 35–73.
[16] P. Zwick, D. Dulić, H. S. J. van der Zant, M. Mayor, *Nanoscale* **2021**, *13*, 15500–15525.
[17] H. Song, M. A. Reed, T. Lee, *Adv. Mater.* **2011**, *23*, 1583–1608.
[18] E. Prats-Alfonso, F. Albericio, *J. Mater. Sci.* **2011**, *46*, 7643–7648.
[19] V. Montes-García, M. A. Squillaci, M. Diez-Castellnou, Q. K. Ong, F. Stellacci, P. Samorì, *Chem. Soc. Rev.* **2021**, *50*, 1269–1304.
[20] S.-W. Choi, H.-S. Kim, W.-S. Kang, J.-H. Kim, Y.-J. Cho, J.-H. Kim, *JNN* **2008**, *8*, 4569–4573.
[21] A. Bauer, W. Schneider, H. Schmidbaur, *Inorg. Chem.* **1997**, *36*, 2225–2226.
[22] M. Basato, G. Facchin, R. A. Michelin, M. Mozzon, S. Pugliese, P. Sgarbossa, A. Tassan, *Inorg. Chim. Acta* **2003**, *356*, 349–356.
[23] W. Schneider, A. Sladek, A. Bauer, K. Angermaier, H. Schmidbaur, *Z. Naturforsch. B* **1997**, *52*, 53–56.
[24] J. Yau, D. M. P. Mingos, *J. Chem. Soc., Dalton Trans.* **1997**, *0*, 1103–1112.
[25] H. Schmidbaur, A. Schier, *Chem. Soc. Rev.* **2011**, *41*, 370–412.
[26] H. Schmidbaur, A. Schier, *Chem. Soc. Rev.* **2008**, *37*, 1931–1951.
[27] T. Mathieson, A. Schier, H. Schmidbaur, *J. Chem. Soc., Dalton Trans.* **2001**, *0*, 1196–1200.
[28] T. J. Mathieson, A. G. Langdon, N. B. Milestone, B. K. Nicholson, *J. Chem. Soc., Dalton Trans.* **1999**, 201–208.
[29] L. M. Bannwart, L. Jundt, T. Müntener, M. Neuburger, D. Häussinger, M. Mayor, *Eur JOC* **2018**, *2018*, 3391–3402.
[30] E. Sidler, P. Zwick, C. Kress, K. Reznikova, O. Fuhr, D. Fenske, M. Mayor, *Chem. Eur. J.* **2022**, *28*, e202201764.
[31] J. E. M. Lewis, J. Winn, L. Cera, S. M. Goldup, *J. Am. Chem. Soc.* **2016**, *138*, 16329–16336.
[32] M. Romain, S. Thiery, A. Shirinskaya, C. Declairieux, D. Tondelier, B. Geffroy, O. Jeannin, J. Rault-Berthelot, R. Métivier, C. Poriel, *Angew. Chem., Int. Ed.* **2015**, *54*, 1176–1180.
[33] K. Reznikova, C. Hsu, W. M. Schosser, A. Gallego, K. Beltako, F. Pauly, H. S. J. van der Zant, M. Mayor, *J. Am. Chem. Soc.* **2021**, *143*, 13944–13951.
[34] J. Norooz Oliaee, M. Dehghany, A. R. W. McKellar, N. Moazzen-Ahmadi, *J. Chem. Phys.* **2011**, *135*, 044315.
[35] E. J. Berquist, J. Clyde, A. Daly, T. Brinzer, K. K. Bullard, Z. M. Campbell, S. A. Corcelli, S. Garrett-Roe, D. S. Lambrecht, *J. Phys. Chem. B* **2017**, *121*, 208–220.
[36] V. P. Dyadchenko, N. M. Belov, M. A. Dyadchenko, Y. L. Slovokhotov, A. M. Banaru, D. A. Lemenovskii, *Russ Chem Bull* **2010**, *59*, 539–543.
[37] H. Schmidbaur, *Nature* **2001**, *413*, 31–33.
[38] H. Schmidbaur, *Chem. Soc. Rev.* **1995**, *24*, 391–400.
[39] P. MacCarthy, *Anal. Chem.* **1978**, *50*, 2165–2165.
[40] D. B. Hibbert, P. Thordarson, *ChemComm* **2016**, *52*, 12792–12805.
[41] P. Thordarson, *Chem. Soc. Rev.* **2011**, *40*, 1305–1323.
[42] C. L. Perrin, T. J. Dwyer, *Chem. Rev.* **1990**, *90*, 935–967.
[43] J. Orts, A. D. Gossert, *Methods* **2018**, *138–139*, 3–25.

Manuscript received: June 28, 2024
Revised manuscript received: July 21, 2024
Accepted manuscript online: July 27, 2024